JMEPEG (2015) 24:4449–4455
DOI: 10.1007/s11665-015-1729-1

1059-9495/$19.00

Corrosion Behavior of Arc-Sprayed Zn-Al Coating in the Presence of Sulfate-Reducing Bacteria in Seawater

Sheng Hong, Yuping Wu, Wenwen Gao, Jianfeng Zhang, and Yujiao Qin

(Submitted April 26, 2015; in revised form August 13, 2015; published online October 9, 2015)

Zn-Al coatings were prepared by high-velocity arc spraying process and were sealed by the silicone resin to improve their corrosion resistance. The corrosion behavior of the unsealed and sealed Zn-Al coatings in the presence of sulfate-reducing bacteria (SRB) in seawater was evaluated, and the related mechanism was discussed. The results showed that the charge transfer resistance value of the sealed coating was almost ten times higher than that of the unsealed coating, and the concentration of element S in the covering layer of the former was half lower than that of the latter. The corrosion resistance of the coating was apparently improved by the sealing treatment. The corrosion rate of the coatings first increased and then decreased during the immersion time of 8 days in the seawater with SRB. The removal of the passive films in the initial period was attributed to penetration of the corrosion medium into the coating and the dissolution of the active zones inside the coating. The adhesion of SRB and accumulation of corrosion products on the coating surface would protect the coating from being further damaged.

Keywords arc spraying, corrosion, sulfate-reducing bacteria Zn-Al coating

1. Introduction

The problem of corrosion is always accompanied by the rapid development of the marine industry, which accounts for enormous economic loss. Recently, much attention has been paid to the corrosion behavior, mechanism and corresponding protection methods of the metal constructions. Among different factors causing the corrosion of marine constructions, microbiologically induced corrosion is the most representative one that closely related to safety incidents and economic losses (Ref 1-4). The sulfate-reducing bacteria (SRB) are ubiquitous microbiology under anaerobic or low dissolved oxygen concentration condition in the marine environment (Ref 5-7). Sulfate acts as a final electron acceptor for the degradation of organism, resulting in the production of sulfide ions, hydrogen sulfide, and sulfides from SRB (Ref 8). According to Iverson's estimation, more than 77% of the corrosion in the producing oil well in America is induced by SRB, which renders the related research urgently needed (Ref 9).

Due to low cost and relatively long service life, zinc, aluminum, or zinc-aluminum alloy coatings by thermal spraying techniques on the metal constructions are effective ways to reduce corrosion damage in the marine environments (Ref 10-12). Arc spraying is a thermal spray process in which an arc is struck between two consumable electrodes of coating materials, and the compressed gas is used to atomize and propel the materials to the substrate. To date, many researches were reported on the fabrication of Zn-Al alloy coatings and the related corrosion mechanism in the marine environments (Ref 13-18). Djerourou et al. (Ref 15) investigated the effects of spray distance on the microstructure and corrosion resistance of arc-sprayed Zn-Al coatings. They found that the coating prepared at spray distance of 100 mm presented higher hardness, low porosity fraction, and better corrosion resistance to seawater solution compared to other prepared coatings. Kroemmer (Ref 16) demonstrated possible ways of improving the corrosion protection of arc-sprayed Zn-Al coatings in the course of a 25-week cyclic aging test as defined in ISO 20340. Kim and Lee (Ref 18) carried out cyclic corrosion tests of arc-sprayed Zn-Al coatings to evaluate their marine corrosion behavior. They showed that the formation of corrosion products such as ZnO and $Zn_5(OH)_8Cl_2 \cdot H_2O$ was observed while oxidation of carbon steel substrates was effectively prevented due to the sacrificial anode effect. Previous investigations mainly considered the influence of Cl^- on the corrosion behavior of arc-sprayed Zn-Al coatings in seawater. However, what is the role that microorganism plays in corrosion process of the coatings is still not clear. In particular, SRB as a ubiquitous microbiology in seawater can cause serious corrosion failure of the coating besides Cl^- due to the effect of the microbial activity.

In the present work, the effects of SRB on the corrosion behavior of arc-sprayed Zn-Al coatings in seawater were studied by using open circuit potential (OCP), electrochemical impedance spectroscopy (EIS), potentiodynamic polarization curves, scanning electron microscopy (SEM), and energy dispersive spectroscopy (EDS). The failure mechanism of the coatings was discussed, and the possible methods to improve their corrosion resistance were proposed.

2. Experimental

2.1 Specimen Preparation

The Q235 steel substrate was cut to produce 10 mm × 10 mm × 5 mm specimens. Its nominal components are listed in

Sheng Hong, Yuping Wu, Wenwen Gao, Jianfeng Zhang, and **Yujiao Qin**, Institute of Metals and Protection, College of Mechanics and Materials, Hohai University, 1 Xikang Road, Nanjing 210098, People's Republic of China. Contact e-mails: wuyuping@hhu.edu.cn and jfzhang@hhu.edu.cn.

Table 1 Chemical composition of the Q235 steel substrate

Element	C	Si	Mn	P	S	Fe
Weight percent (wt.%)	0.14 to 0.22	≤ 0.35	≤ 0.14	≤ 0.045	≤ 0.05	Balance

Table 1. Zn-Al wire, containing 85% Zn and 15% Al (mass fraction) and 3 mm in diameter, was selected as the spraying material wire. Prior to spraying, all the surfaces of steel substrate were cleaned in acetone and then sandblasted using corundum powder. A CD-500 arc spraying system was used to deposit the coatings with the parameters of spray voltage as 32 V, spray current as 100 A, spray distance as 200 mm, and air pressure as 0.65 MPa. The total thickness of the coatings was controlled by the number of passes of the spray gun. The coatings were built up to a thickness of 160 ± 20 μm. After the coating process, a group of specimens were sealed in a mold of silicone resin.

2.2 The Culture of SRB and Test Medium

The SRB was obtained from muddy sediment in Jiaozhou Bay of Qingdao. Fresh marine sediment was added into a sterile modified Postgate's C (PGC) medium to enrich anaerobic bacteria. The bacteria were subsequently purified in sterile agar plates by picking up several single colonies with a sterile inoculation loop. The procedure was repeated until the colonies of single SRB strain were formed on the solid PGC medium. The modified Postgate's C culture solution contained 0.5 g KH_2PO_4, 1 g NH_4Cl, 0.06 g $CaCl_2{\cdot}6H_2O$, 0.06 g $MgSO_4{\cdot}7H_2O$, 6 mL 70% sodium lactate, 1 g yeast extract, and 0.3 g sodium citrate in 1 L seawater from Qingdao offshore area. The pH value was adjusted to 7.0 using the appropriate amount of sodium hydroxide before the medium was autoclaved at 121 °C for 20 min.

2.3 Electrochemical Tests

Before tests, working electrode, counter electrode, rubber stoppers, and salt bridge were degreased with ethanol using an ultrasonic bath followed by exposure to a UV lamp for 20 min. All electrochemical experiments were performed at 30 °C.

All the electrochemical tests were carried out using the Solartron SI1287 electrochemical interface and SI1260 impedance/gain phase analyzer control systems. The electrodes used were as follows: a working electrode, a Ruthenium-titanium counter electrode, and a silver/silver chloride (Ag/AgCl, 3 M KCl) reference electrode (CH Instruments, Inc.). The EIS data were measured at OCP with sine wave voltages (10 mV) peak to peak in a frequency range of 100 kHz to 10 mHz. The experimental data were interpreted on the basis of equivalent analogs using the software ZsimpWin3.21 to obtain the fitting parameters. The potentiodynamic polarization curves were carried out from −400 to 400 mV versus OCP with a fixed sweep rate of 0.5 mV s^{-1}. Each test was repeated at least thrice to make sure a good repeatability of the experiment result.

2.4 Surface Analysis

The samples were immersed for 2 h in a 5% glutaraldehyde solution in order to fix the bacteria on their surface, and then they were sequentially dehydrated through a graded series of ethanol solutions (15 min each): 50, 75, and 100%. The microstructures of the samples were characterized by scanning electron microscopy (SEM) and electron dispersive spectroscopy (EDS) analysis, respectively.

3. Results and Discussion

3.1 Coating Microstructure

Arc-sprayed coatings were built up by splat with particles impacting on those already solidified during the spraying process, which had a highly anisotropic and layered structure with a certain amount of micro-cracks and pores. The structural defects would be preferential corrosion initiation sites, providing diffusion channels for electrolytes from the outer surface to the interior and deteriorating the corrosion resistance of the coating. Therefore, it is necessary to conduct sealing treatment for arc-sprayed coatings in practical applications. In this experiment, the silicone resin was used as sealing agent due to its superior flowability and permeability.

Figure 1(a) and (b) shows the surface morphologies of the coating before and after sealing, respectively. It can be seen that roughness and porosity of the coating were greatly reduced after sealing. In addition, open cracks and pores in the coating were filled with silicone resin, leading to the improvement of surface quality and the reduction in the initiation sites of corrosion damage. This would improve the corrosion resistance of the coating.

3.2 Open Circuit Potential

Figure 2 shows the E_{ocp} obtained for both unsealed and sealed Zn-Al coating versus immersion time in SRB culture solution during a growth cycle. Under the unsealed condition, the E_{ocp} shifted in a direction from −994 to −1022 mV during first 24 h. The fall of the potential could be attributed to the corrosion medium (Cl^- and metabolites of the SRB, including S^{2-}, H_2S, organic acids, etc.) penetrated into the coating, which caused the dissolution of the active zones inside the coating (Ref 19, 20). After 24 h, the E_{ocp} shifted slowly in a positive direction from −1022 to −983 mV. This can be due to (a) the corrosion products, such as zinc sulfide, plugged the pore in the coating, (b) the adhesion of SRB and the accumulation of corrosion products on the coating surface hindered the corrosion medium into the coating (Ref 21, 22). Under the sealed condition, the E_{ocp} shifted in a positive direction from −985 to −948 mV during first 48 h. It can be due to the adsorption of the SRB and corrosion products on the sealed coating surface (Ref 22). After 48 h, the E_{ocp} reached an almost constant value of −945 mV, which indicated the kinetics of electrochemical processes of the sample surface was relatively stable. In addition, the E_{ocp} value of sealed Zn-Al coating was always higher than that of unsealed one during the whole experiment processes, which meant that unsealed Zn-Al coating had more greatly corrosion tendency than that of sealed Zn-Al coating.

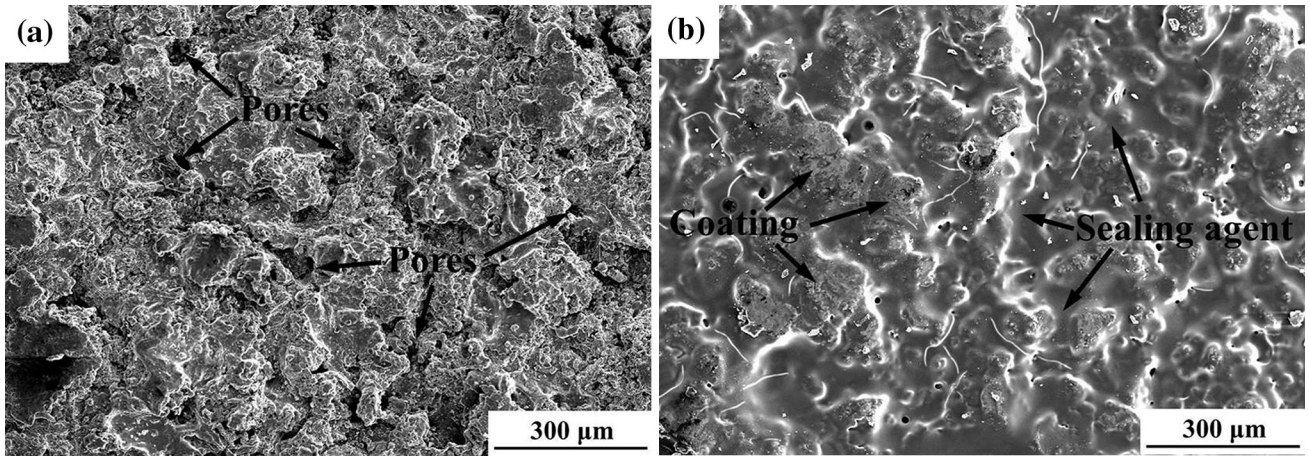

Fig. 1 The surface morphology of Zn-Al coatings: (a) unsealed (b) sealed

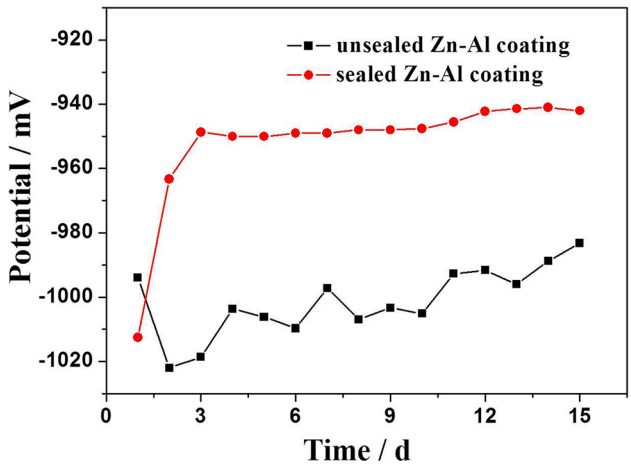

Fig. 2 Time dependence of E_{ocp} for Zn-Al coatings under unsealed and sealed conditions in seawater with SRB

3.3 Electrochemical Impedance Spectroscopy

Figure 3 shows the Nyquist plots of unsealed (a) and sealed (b) Zn-Al coatings after immersion for 1-15 days in seawater with SRB. The results of EIS were analyzed using ZsimpWin software; the quality of the fit to the equivalent circuit was based on the sum of the square of the differences between the experimental data and the fitting results. Moreover, the average variance χ^2 value reached the level of 10^{-3} (Ref 23). The equivalent circuits describing the electrochemical reaction for unsealed and sealed Zn-Al coatings are shown in Fig. 4.

According to the characteristic of Nyquist plots of unsealed Zn-Al coating after immersion for 1 day and sealed Zn-Al coating after immersion for 1 to 15 days, the equivalent circuit of two time constants (Fig. 4(a)) was used to fit the EIS data. A constant phase element (CPE) is commonly used to replace capacitance, because it has hardly a pure capacitance in a real electrochemical process (Ref 24). The presence of CPE can be interpreted by dispersion effects that attributed to the surface roughness of the sample. The

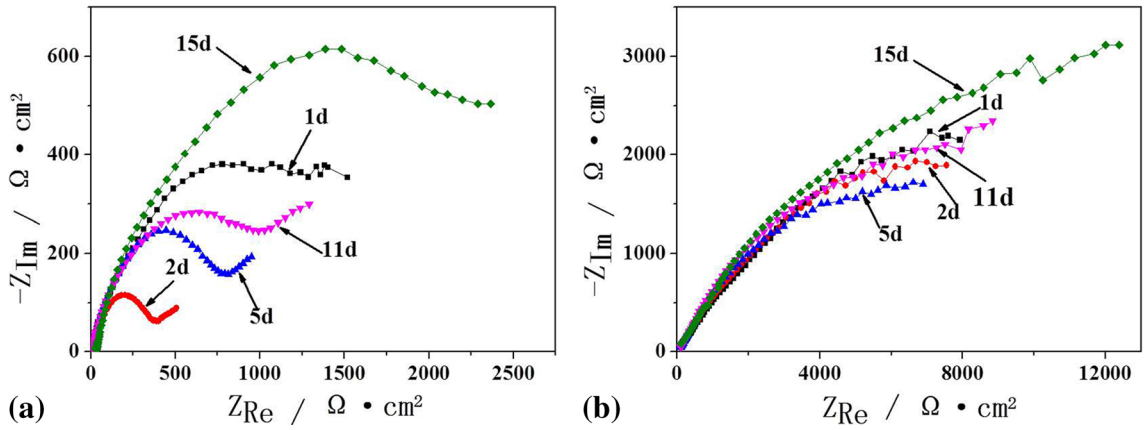

Fig. 3 The impedance plots of Zn-Al coatings under unsealed (a) and sealed (b) conditions in seawater with SRB

CPE impedance is described as $Z_{CPE} = Y_o(jw)^{-n}$ $(0 < n < 1)$, where n is an empirical exponent, the value of n can reflect the degree of heterogeneities on the sample surface (Ref 20). In this case, R_s, R_p, R_{ct}, CPE_{-c}, and CPE_{-ct} represent the solution resistance, the resistance of pores, the charge transfer resistance of the coating/substrate interface, the capacitance of the coating, and the capacitance of the double layer, respectively. A pair of elements in parallel, namely CPE_{-c} and R_p, represents the dielectric properties of the coating. Another pair of CPE_{-ct} and R_{ct} in parallel is adopted to describe the electrochemical reaction process at the coating/substrate interface.

Increasing the immersion time from 2 to 15 days, the style of the Nyquist plots of unsealed Zn-Al coating was changed. A straight line appeared at low frequency, suggesting that Warburg impedance occurred when mass-transfer reaction was influenced by the accumulation of the corrosion products in the pore (Ref 25). The equivalent circuit in Fig. 4(b) was used to fit the Nyquist plots of unsealed Zn-Al coating after immersion for 2 to 15 days, which consisted of an additional element Warburg impedance (Z_w) compared to the equivalent circuit in Fig. 4(a), a parameter containing diffusion coefficient and characteristic of stagnant layer.

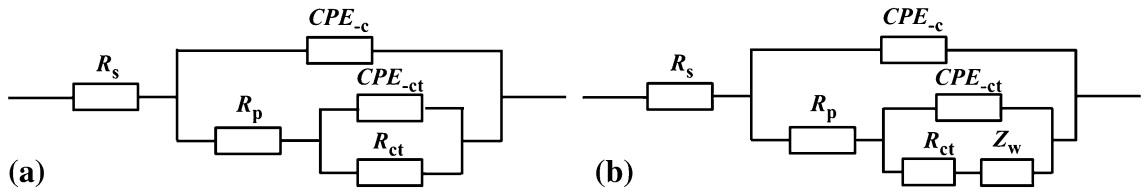

Fig. 4 Equivalent circuit for Zn-Al coatings under unsealed (a, b) and sealed (a) conditions in seawater with SRB

Table 2 Parameters of EIS for the unsealed Zn-Al coatings in SRB solution after immersion for different times

Time, days	R_s, Ω cm^2	CPE_{-c}, F cm^{-2}	n_1	R_p, Ω cm^2	CPE_{-ct}, F cm^{-2}	n_2	R_{ct}, Ω cm^2	Z_w
1	14.9	4.45×10^{-5}	0.667	1.54×10^{2}	4.19×10^{-4}	0.793	1.68×10^{3}	
2	13.2	2.93×10^{-4}	0.839	1.10×10^{2}	6.16×10^{-5}	1.00	2.23×10^{2}	0.0256
5	15.7	3.27×10^{-4}	0.629	1.98×10^{2}	5.82×10^{-5}	0.809	7.93×10^{2}	0.0170
11	18.5	3.45×10^{-4}	0.458	2.78×10^{2}	3.15×10^{-5}	0.739	1.18×10^{3}	0.0246
15	29.6	2.12×10^{-4}	0.685	2.87×10^{2}	1.03×10^{-5}	0.689	1.91×10^{3}	0.0252

Table 3 Parameters of EIS for the sealed Zn-Al coatings in SRB solution after immersion for different times

Time, days	R_s, Ω cm^2	CPE_{-c}, F cm^{-2}	n_1	R_p, Ω cm^2	CPE_{-ct}, F cm^{-2}	n_2	R_{ct}, Ω cm^2
1	28.5	1.85×10^{-5}	0.418	2.19×10^{3}	3.32×10^{-4}	0.584	1.23×10^{4}
2	19.4	1.61×10^{-4}	0.371	1.39×10^{3}	1.24×10^{-4}	0.660	1.15×10^{4}
5	25.7	1.50×10^{-4}	0.342	1.25×10^{3}	7.78×10^{-5}	0.691	1.07×10^{4}
11	23.4	1.15×10^{-4}	0.341	1.68×10^{3}	3.44×10^{-5}	0.727	1.25×10^{4}
15	32.5	7.39×10^{-5}	0.358	2.33×10^{3}	2.59×10^{-5}	0.803	1.39×10^{4}

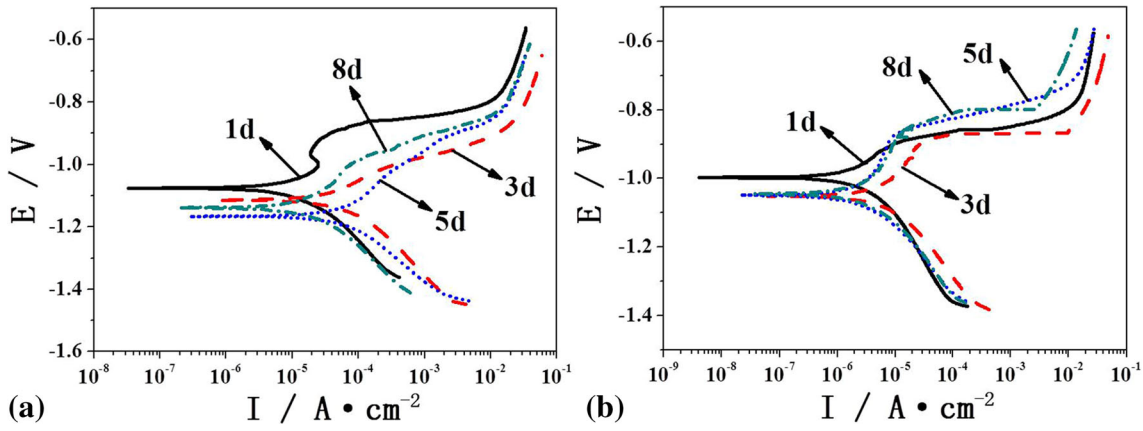

Fig. 5 Potentiodynamic polarization curves of Zn-Al coatings under unsealed (a) and sealed (b) conditions in seawater with SRB

Table 4 Analysis parameters of potentiodynamic polarization curve of unsealed and sealed Zn-Al coatings in seawater with SRB

	E_{corr}, V		i_{corr}, A cm^{-2}	
Time, days	Unsealed	Sealed	Unsealed	Sealed
1	−1.08	−0.997	6.40×10^{-6}	3.31×10^{-6}
3	−1.12	−1.05	2.73×10^{-5}	5.92×10^{-6}
5	−1.17	−1.05	1.65×10^{-5}	4.03×10^{-6}
8	−1.14	−1.04	1.08×10^{-5}	3.69×10^{-6}

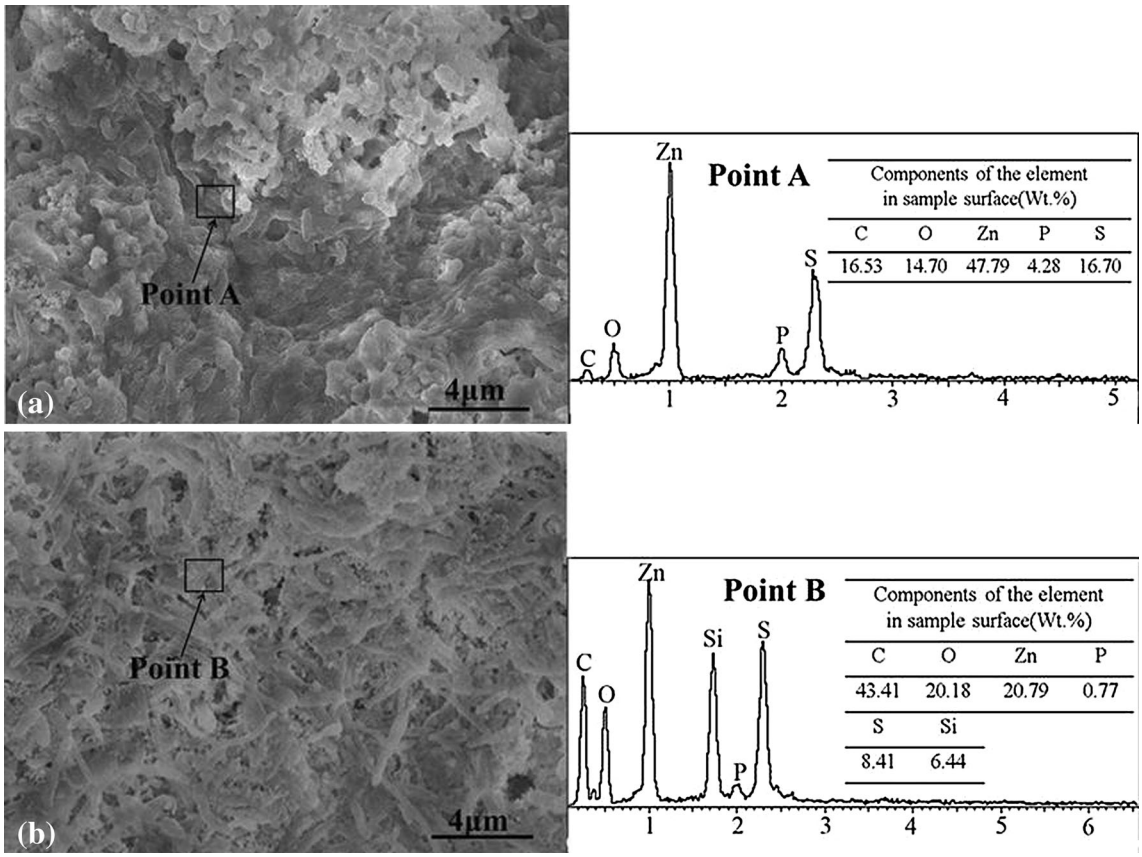

Fig. 6 SEM and EDS analysis for Zn-Al coatings under unsealed (a) and sealed (b) conditions in seawater with SRB

To compare the corrosion resistance of Zn-Al coatings with and without sealing, typical electrochemical corrosion parameters extracted from the fitting equivalent circuit for unsealed and sealed Zn-Al coatings are listed in Tables 2 and 3, respectively. As shown in Table 2, the R_p and R_{ct} values of unsealed Zn-Al coatings decreased during the first 2 days, which was attributed to penetration of the corrosion medium (Cl^- and the metabolites of SRB, including S^{2-}, H_2S, organic acids, etc.) into the coating continuously through the pore and microcracks and the dissolution of the active zones inside the coating (Ref 26). The R_p and R_{ct} values increased with increasing the immersion to 15 days. This is because the ion mass transfer via the coating defects was restricted (Ref 27). The galvanic pair was formed between the steel substrate and coating, which was probably due to the coating was nobler than the steel substrate. When corrosion attack occurred preferentially in the coating, the formation of the corrosion products in the permeable channels could not be completely transferred and diffused into solution, and some of the corrosion products plugged the channels, which was called "plugging effect" (Ref 28). Meanwhile, the adhesion of SRB and the accumulation of corrosion products on the coating surface would hinder the penetration of the corrosion medium into the coating.

The R_p and R_{ct} values of sealed Zn-Al coatings show a similar trend (as can be seen in Table 3). The R_p and R_{ct} values decreased during the first 5 days, indicating that the localized corrosion occurred on the sealed coating surface due to the heterogeneity after sealing. Then the values increased with increasing the immersion to 15 days. This could also be attributed to the adhesion of SRB and the accumulation of corrosion products on the coating surface.

Comparing the R_{ct} values in Tables 2 and 3, it can be seen that the corrosion resistance of the sealing Zn-Al coating was much larger than that of the unsealed Zn-Al coating. It may be suggested that the sealants prevented the corrosion medium from penetrating into the coating and reduced the corrosion rate after appropriate sealing treatment.

3.4 Tafel Polarization Tests

The potentiodynamic polarization curves of unsealed and sealed Zn-Al coatings in SRB solution at static condition for different times are shown in Fig. 5(a) and (b), respectively. The corrosion potential (E_{corr}) and corrosion current density (i_{corr}) extracted from the curves are shown in Table 4.

As shown in Table 4, the i_{corr} of the unsealed and sealed coatings both increased to the maximum values after immersion for 3 days, and then decreased continuously with increasing the immersion to 8 days. This could be attributed to the combined effects of Cl^- and the metabolites of SRB. The removal of the passive films in the initial period by the corrosion medium would accelerate the corrosion process. However, the adhesion of SRB and accumulation of corrosion products on the coating surface protected the coating from being further damaged. Thus, the corrosion rate of the coatings first increased and then decreased during the immersion time of 8 days in the seawater with SRB.

The i_{corr} of the sealed Zn-Al coating was lower than that of the unsealed Zn-Al coating, suggesting that the sealing treatment decreased the corrosion rate and thus enhanced the corrosion resistance of the Zn-Al coating apparently by reducing the porosity inside the coating and retarding the penetration of the corrosion medium into the Zn-Al coating (Ref 29).

3.5 Surface Analysis

Figure 6 shows the SEM and EDS analysis of unsealed (a) and sealed (b) Zn-Al coatings in SRB solution after immersion for 15 days. A covering layer which was constituted by the SRB and corrosion products can be seen on the unsealed Zn-Al coating surface in Fig. 6(a). While in Fig. 6(b), a large amount of SRB was attached on the sealed Zn-Al coating surface. Moreover, some floccules were found among the SRB biofilms, which were supposed to be corrosion products by the interaction between the coating and the metabolites of SRB. It can be seen from Fig. 6 that the covering layer on the sealed Zn-Al coating surface was more homogeneous than that of unsealed Zn-Al coating, while the structure of the covering layer on the sealed Zn-Al coating surface was more loose. The EDS analysis of both point A and B indicated that the covering layer of the coating immersed in SRB solution was composed of C, O, Zn, P, and S. However, the Al element was not detected due to its low content. It is considered that the main component of the corrosion products was ZnS. Comparing the elements concentration of both point A and B, it can be seen that the concentration of S and Zn in the covering layer under the sealed condition was smaller than that under unsealed condition, suggesting that the corrosion level under unsealed condition was more severe than that under sealed condition. It demonstrated that the surface analysis was consistent with the results of electrochemical tests.

4. Conclusions

(1) In the early stage of immersion process, the sulfate-reducing bacteria (SRB) caused the corrosion of arc-sprayed Zn-Al coatings mainly by the metabolites. In the middle and later stages of immersion process, the production dissolved from the coating in the corrosive medium reacted with S-containing metabolism of SRB, and thus generated corrosion product of ZnS to plug the pores in the coating.

(2) The pores in the coating had a significant effect on the corrosion resistance, i.e., the larger was the porosity, the worse was the corrosion resistance. Sealing treatment can significantly improve the ability of the coating to resist the corrosive attack by seawater.

(3) In seawater with SRB, corrosion protection of the steel substrate by arc-sprayed Zn-Al coating mainly depended on cathodic protection and sealing effect of corrosion products.

Acknowledgments

The research was supported by the National Natural Science Foundation of China (Grant No. 51579087), the Natural Science Foundation of Jiangsu Province of China (Grant No. BK20150806) and the Fundamental Research Funds for the Central Universities (Grant Nos. 2013B34414 and 2015B01514). Professor Jizhou Duan of Institute of Oceanology, Chinese Academy of Sciences was also acknowledged for providing microbiologically induced corrosion equipment.

References

1. L.L. Machuca, S.I. Bailey, and R. Gubner, Systematic Study of the Corrosion Properties of Selected High-Resistance Alloys in Natural Seawater, *Corros. Sci.*, 2012, **64**, p 8
2. S.C. Dexter, Role of Microfouling Organisms in Marine Corrosion, *Biofouling*, 1993, **7**, p 97
3. L.L. Machuca, R. Jeffrey, S.I. Bailey, R. Gubner, E. Watkin, M.P. Ginige, A.H. Kaksonen, and K. Heidersbach, Filtration-UV Irradiation as an Option for Mitigating the Risk of Microbiologically Influenced Corrosion of Subsea Construction Alloys in Seawater, *Corros. Sci.*, 2014, **79**, p 89
4. L.L. Machuca, S.I. Bailey, R. Gubner, E. Watkin, A. Kaksonen, and K. Heidersbach, Effect of Oxygen and Biofilms on Crevice Corrosion of UNS S31803 and UNS N08825 in Natural Seawater, *Corros. Sci.*, 2013, **67**, p 242
5. S. Paisse, J.F. Ghiglione, F. Marty, B. Abbas, H. Gueune, J. Amaya, J. Maria, G. Muyzer, and L. Quillet, Sulfate-Reducing Bacteria Inhabiting Natural Corrosion Deposits from Marine Steel Structures, *Appl. Microbiol. Biotechnol.*, 2013, **97**, p 7493
6. N.D. Gungor, A. Cotuk, and D. Dispinar, The Effect of desulfovibrio sp. Biofilms on Corrosion Behavior of Copper in Sulfide-Containing Solutions, *J. Mater. Eng. Perform.*, 2015, **24**, p 1357
7. Y. Wan, D. Zhang, H.Q. Liu, Y.J. Li, and B.R. Hou, Influence of Sulfate-Reducing Bacteria on Environmental Parameters and Marine Corrosion Behavior of Q235 Steel in Aerobic Conditions, *Electrochim. Acta*, 2010, **55**, p 1528
8. G. Muyzer and A.J.M. Stams, The Ecology and Biotechnology of Sulfate-Reducing Bacteria, *Nat. Rev. Microbiol.*, 2008, **6**, p 441
9. W.P. Iverson, *Adv. Corros. Sci. Technol.*, 1972, **2**, p 1
10. Q. Jiang, Q. Miao, F. Tong, Y. Xu, B.L. Ren, Z.M. Liu, and Z.J. Yao, Electrochemical Corrosion Behavior Of Arc Sprayed Al-Zn-Si-RE Coatings on Mild Steel in 3.5% NaCl Solution, *Trans. Nonferrous Met. Soc. China*, 2014, **24**, p 2713
11. S. Kuroda, J. Kawakita, and M. Takemoto, An 18-year Exposure Test of Thermal-Sprayed Zn, Al, and Zn-Al Coatings in Marine Environment, *Corrosion*, 2002, **62**, p 635
12. F. Ahnia and B. Demri, Evaluation of Aluminum Coatings in Simulated Marine Environment, *Surf. Coat. Technol.*, 2013, **220**, p 232
13. Q. Jiang, Q. Miao, W.W. Liang, F.G. Ying, F. Tong, Y. Xu, B.L. Ren, Z.J. Yao, and P.Z. Zhang, Corrosion Behavior of Arc Sprayed Al-Zn-Si-RE Coatings on Mild Steel in 3.5 wt.% NaCl Solution, *Electrochim. Acta*, 2014, **115**, p 644
14. D.X. Fu, B.S. Xu, W. Zhang, S.C. Wei, and Y. Liu, Failure Mechanism of Organic Coatings Overlaid on Arc Sprayed Coatings, *Surf. Eng.*, 2009, **25**, p 612
15. S. Djerourou, H. Lahmar, N. Bouhellal, and Y. Mebdoua, Study of Twin Wire Arc Sprayed Zinc/Aluminum Coating on Low Carbon Steel Substrate: Application to Corrosion Protection, *Adv. Mater. Res.*, 2013, **685**, p 271

16. W. Kroemmer, High Performance Arc Sprayed Coatings for Active Corrosion Protection in Offshore Applications, *Proceedings of the International Thermal Spray Conference*, 2013, p 97
17. W.M. Zhao, Y. Wang, C. Liu, L.X. Dong, H.H. Yu, and H. Ai, Erosion-Corrosion of Thermally Sprayed Coatings in Simulated Splash Zone, *Surf. Coat. Technol.*, 2010, **205**, p 2267
18. J.H. Kim and M.H. Lee, A Study on Cavitation Erosion and Corrosion Behavior of Al-, Zn-, Cu-, and Fe-Based Coatings Prepared by Arc Spraying, *J. Therm. Spray Technol.*, 2010, **19**, p 1224
19. Y. Wang, W. Tian, T. Zhang, and Y. Yang, Microstructure, Spallation and Corrosion of Plasma Sprayed Al_2O_3-13%TiO_2 Coatings, *Corros. Sci.*, 2009, **51**, p 2924
20. F.L. Liu, J. Zhang, S. Zhang, W.H. Li, J.Z. Duan, and B.R. Hou, Effect of Sulfate Reducing Bacteria on Corrosion of Al-Zn-In-Sn Sacrificial Anodes in Marine Sediment, *Mater. Corros.*, 2012, **63**, p 431
21. C. Liu, Q. Bi, and A. Matthews, EIS Comparison on Corrosion Performance of PVD TiN and CrN Coated Mild Steel in NaCl Aqueous Solution, *Corros. Sci.*, 2001, **43**, p 1953
22. S. Cheng, J.T. Tian, S.G. Chen, Y.H. Lei, X.T. Chang, T. Liu, and Y.S. Yin, Microbially Influenced Corrosion of Stainless Steel by Marine Bacterium *Vibrio natriegens*: (I) Corrosion Behavior, *Mater. Sci. Eng. C*, 2009, **29**, p 751
23. J.S. Rodríguez, F.S. Hernández, and J.G. González, Comparative Study of the Behaviour of AISI, 304 SS in a Natural Seawater Hopper, in Sterile Media and with SRB Using Electrochemical Techniques and SEM, *Corros. Sci.*, 2006, **48**, p 1265
24. Y.J. Qin, Y.P. Wu, J.F. Zhang, W.M. Guo, S. Hong, and L.Y. Chen, Long-Term Corrosion Behavior of HVOF Sprayed FeCrSiBMn Amorphous/Nanocrystalline Coating, *Trans. Nonferrous Met. Soc. China*, 2015, **25**, p 1144
25. M.M. Verdian, K. Raeissi, and M. Salehi, Corrosion Performance of HVOF and APS Thermally Sprayed NiTi Intermetallic Coatings in 3.5% NaCl Solution, *Corros. Sci.*, 2010, **52**, p 1052
26. E.A. Esfahani, H. Salimijazi, M.A. Golozar, J. Mostaghimi, and L. Pershin, Study of Corrosion Behavior of Arc Sprayed Aluminum Coating on Mild Steel, *J. Therm. Spray Technol.*, 2012, **21**, p 1195
27. X.D. Zhao, J.Z. Duan, B.R. Hou, and S.R. Wu, Effect of Sulfate-Reducing Bacteria on Corrosion Behavior of Mild Steel in Sea Mud, *J. Mater. Sci. Technol.*, 2007, **23**, p 323
28. M. Campo, M. Carboneras, M.D. López, B. Torres, P. Rodrigo, E. Otero, and J. Rams, Corrosion Resistance of Thermally Sprayed Al and Al/SiC Coatings on Mg, *Surf. Coat. Technol.*, 2009, **203**, p 3224
29. J.J. Zhang, Z.H. Wang, P.H. Lin, L.Q. Si, G.J. Shen, Z.H. Zhou, S.Q. Jiang, and W.H. Lu, Corrosion of Plasma Sprayed NiCrAl/Al_2O_3-13 wt.%TiO_2 Coatings with and Without Sealing, *Surf. Eng.*, 2012, **28**, p 345